EasyChair Preprint

№ 2037

Characteristics Measurement of Baghdad University Radio Telescope for Hydrogen Emission Line

Uday Jallod and Kamal Abood

November 26, 2019

Characteristics Measurement of Baghdad University Radio Telescope for Hydrogen Emission Line

Uday E. Jallod[a)], and Kamal M. Abood[b)]

Astronomy and Space Department, College of Science, University of Baghdad, Baghdad, Iraq

[a)]udayjallod@scbaghdad.edu.iq
[b)]kamalabood@scbaghdad.edu.iq

Abstract. The aim of this paper is to measure the characteristics properties of 3 m radio telescope that installed inside Baghdad University campus. The measurements of this study cover some of the fundamental parameters at 1.42 GHz. These parameters concentrated principally on, the system noise temperature, signal to noise ratio and sensitivity, half power beam width, aperture efficiency, and effective area. These parameters are estimated via different radio sources observation like Cas-A, full moon, sky background, and solar drift scan observations. From the results of these observations, these parameters are found to be approximately 64 K, 1.2, 0.9 Jansky, 3.7°, 0.54, and 3.8 m^2 respectively. The parameters values have vital affect to quantitative assessment of our radio telescope and they are in a good correlation with the results presented in the literature.

INTRODUCTION

Several types of spectral emission lines are observed by radio astronomers, but the most important of them is the hydrogen radio emission line. The detection of this line was made in 1951 by Ewen and Purcell [1]. This line is emitted via the hyperfine spin-flip transition of neutral atomic hydrogen at frequency near 1.42 GHz (21 cm wavelength) which is located within L band frequency (1 – 2) GHz [2]. Most of the radio emission processes occurring on stars have probably been identified from solar studies [3]. Nowadays, modern solar radio astronomy is taken the next step in advanced our knowledge of the sun. The solar radio emissions could be considered complex, and it shows variations over a range of temporal scales ranging from sub millisecond to solar cycles. Solar hydrogen emission line is available and its unique frequency, allow astronomers to record it from the ground by small radio telescopes. Consequently, most solar radio observations come from single dish instruments. These observations could provide details about evolution of the solar emissions, but cannot provide any information of the morphology or location of emissions [4].

In hydrogen spectral line mode many adjacent frequency channels are required within one band to determine the shape of an astronomical object spectrum whose brightness changes rapidly with frequency. So, the receiver spectrometer is divided into many frequency channels to observe emission lines. These channels are equal width and measure the power simultaneously, usually via digital signal processing [5]. The observed spectrum provides the astronomers a useful information about the nature of the physical processes that producing the emissions [6].

All higher angular resolution observations are made using ground based telescopes, because of large aperture telescopes are only possible at present from the ground. On the ground, radio telescopes are easier to operate, maintain, and could be adjustment preparation and modification [7]. There are several parameters that control a radio telescope performance, such as system noise temperature, signal to noise

ratio, sensitivity, beam width of radiation pattern, efficiency, and effective area. A literary review of basic and existing of radio telescope antenna types was done in several studies [8]. Recently, new types of antenna have been proposed to be used in radio telescope system. The basic antenna types such as dipole, horn, helical, micro – strip, and parabolic reflector antenna [9]. A parabolic antenna could be classified as small, medium, large, and ultra large. A small antenna whose aperture smaller than 10 m of diameter, a medium antenna whose aperture is from (10 - 30) m of diameter, large antenna whose aperture 100 m of diameter, and more than 100 m is called ultra large [10]. In our study, the characteristics of fundamental parameters that related to Baghdad University Radio Telescope (BURT) are measured like, the system noise temperature, signal to noise ratio and sensitivity, half power beam width, aperture efficiency, and effective area. These parameters are measured at 1.42 GHz by different radio sources observation. Cas-A, full moon, sky background, and sun drift scan observations have been observed to estimate the values of these parameters.

FUNDAMENTAL THEORETICAL CONCEPTS

The receiver total temperature (T_{tot}) could be given by [11]:

$$T_{tot} = T_A + T_{sys} \quad (1)$$

where T_A is the antenna temperature due to an observed source, and T_{sys} is the system noise temperature. T_{sys} describes the amount of noise added by the station hardware to the received signal. T_{sys} is a critical factor in determine Signal to Noise Ratio (*SNR*), and sensitivity. T_{sys} could be given as [12]:

$$T_{sys} = T_{cmb} + T_{wv} + T_g + T_{at} + T_r \quad (2)$$

where T_{cmb} is the cosmic microwave background, T_{wv} is the radiation from water vapor in atmosphere, T_g is the radiation from the ground, T_{at} is the radiation from the atmosphere, and T_r is receiver noise temperature.

SNR is given by [13]:

$$SNR = \frac{T_A}{T_{sky}} \quad (3)$$

where T_{sky} is the sky background temperature.

The sensitivity of a radio telescope could be expressed as the minimum detectable flux density (s_{min}), and could be written as [14]:

$$s_{min} = \frac{3kT_{sys}}{A_e}\frac{1}{\sqrt{\Delta\nu\tau}} \quad (4)$$

where k is Boltzmann constant, A_e is the effective area of an antenna, $\Delta\nu$ is the bandwidth frequency of the telescope radiometer in Hz, and τ is the integration time (second).

The radio telescope receives a radiation from a radio source in a solid angle that is called the beam of the antenna. The resolution of the telescope is determined by the Half Power Beam Width (θ_{HPBW}) that given by diffraction theory to be [15]:

$$\theta_{HPBW} = 1.028\frac{\lambda}{D} \quad (5)$$

where λ is the observed wavelength and D is the diameter of the antenna.

Using the Nyquist theorem, could be introduce T_A by [16]:

$$T_A = \frac{P_A}{k\Delta v} \tag{6}$$

where p_A is the antenna received power. If the observed discrete source whose angular size small compared to the antenna solid angle (Ω_A) with a constant source brightness temperature (T_B) and accuracy pointed antenna, this leads to [17]:

$$T_A = T_B \frac{\Omega_s}{\Omega_A} \tag{7}$$

where Ω_s is the solid angle subtended by the source. Then the flux density of a radio source is calculated using measured T_A according to [18]:

$$s = \frac{2kT_A}{\eta A} \tag{8}$$

where η is the aperture efficiency, and A is the physical aperture area, η could be given as [19]:

$$\eta = \frac{A_e}{A} \tag{9}$$

OBSERVATIONS AND RESULTS

The observations are carried out using Baghdad University Radio Telescope (BURT). This telescope has diameter (D = 3 m), focal length (f = 1.18 m) and f/D ratio is 0.39. Our measurements are (T_{sys}, SNR, s_{min}, θ_{HPBW}, η, and A_e) parameters. The research procedure as a block diagram is described in Fig. (1).

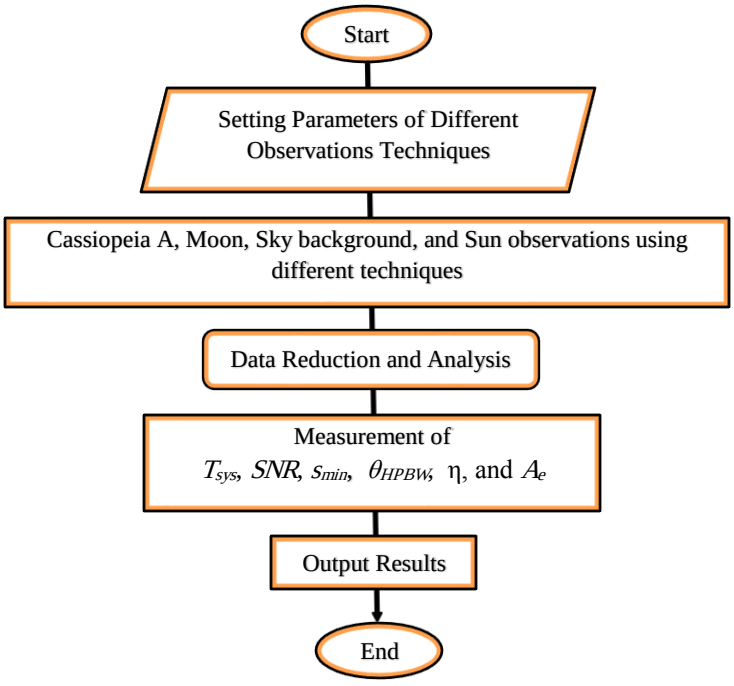

FIGURE 1: The block diagram represents the methodology of our study

T_{sys} could be calculated from well-known source like Cassiopeia-A (Cas-A) source. Cas-A is the remnant of supernova explosion in our galaxy at distance 3 kpc, and has a very stable flux density about 2477 Jansky (Jy) in 1.42 GHz [20]. This source is used to measure T_{sys}. The antenna is pointed to the Cas-A position then the antenna remained less than five minutes on the direction of the source. This time is chosen to ensure the source inside the beam width of our radio telescope antenna. Sky background noise was estimated by moving the antenna to another position in order to ensure there is no signal comes from the source where the telescope is moved by separation distance of 50° in azimuth (ϕ) with the same elevation (θ). This estimation is then subtracted from our observation in order to avoid the unwanted noise error. It should be pointed out here that the sky background noise is also recorded within five minutes in order to maintain the signal and noise observations to be in the same size. Cas-A, moon, and sky background are observed using radio telescope spectrometer. The spectrometer parameters are span, sweep time, center frequency, Resolution Bandwidth (RBW), and Video Bandwidth (VBW) as displayed in table 1.

TABLE 1: Source position, observation date, and selecting parameters values of the radio telescope spectrometer.

Source	**Antenna Position**	**Date**	**Local Time**	**Input Value Of Spectrometer Parameters**				
Cas-A	ϕ=200° θ =55°	12-2-2019	9:26 AM	Center Freq. (Hz)	Sweep Time (Sec.)	Span (Hz)	RBW (Hz)	VBW (Hz)
Sky Background	ϕ =250° θ =55°	12-2-2019	9:48 AM					
Moon	ϕ = 55° θ = 22°	20-3-2019	6:45 PM	1.42×109	30	2×10^7	10^5	10
Sky Background	ϕ =55° θ =70°	20-3-2019	6:55 PM					

The simplest procedure to measure T_{sys} could be estimated by making two observations. The first include the source in the beam (power on (p_{on}) or ($T_{A\text{-}on}$)) and the second is exclude the source (power off (p_{off}) or ($T_{A\text{-}off}$)), where $T_{A\text{-}on}$ is the antenna temperature due to an observed source, and $T_{A\text{-}off}$ is antenna temperature due to sky background, as given by Y ratio [21]:

$$Y = \frac{p_{on}}{p_{off}} = \frac{T_{A-on}+T_{sys}}{T_{A-off}+T_{sys}} \qquad (10)$$

Eq. (10) could be written as,

$$T_{sys} = \frac{T_{A-on}-Y\times T_{A-off}}{Y-1} \qquad (11)$$

The results of Cas-A and sky background observations are shown in Fig. (2).

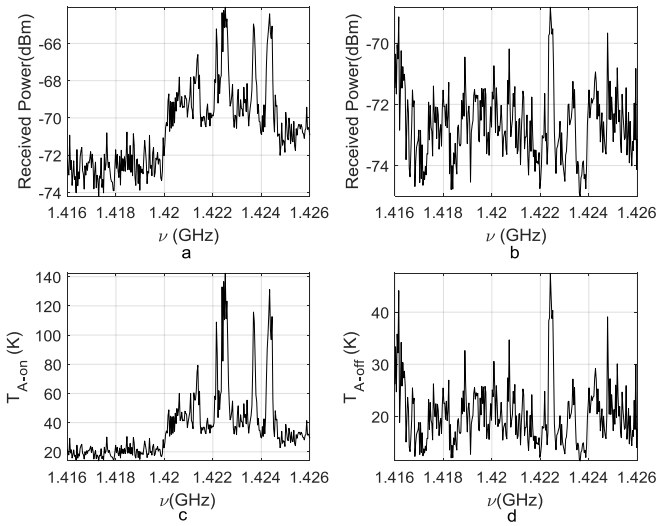

FIGURE 2: Received power (dBm) as a function of frequency *v* (GHz): a- Cas-A source observation, b- sky background observation. c-$T_{A\text{-on}}$ (K) due to the Cas-A, d -$T_{A\text{-off}}$ (K) due to the sky background.

Y ratio is then computed via eq. (10) and found to be (0.95 dB), or (*Y*= 1.24), then T_{sys} is approximately found to be 64 K according to eq. (11).

T_A could be estimated as follow [12]:

$$T_A = T_{A-on} - T_{A-off} \tag{12}$$

and the result is displayed in Fig. (3).

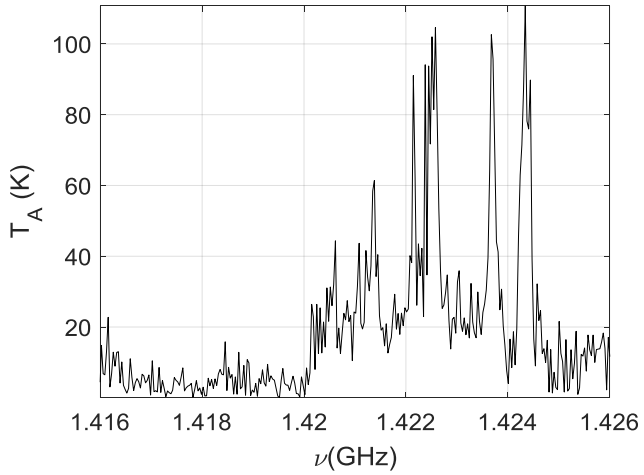

FIGURE 3: The result of subtracted Fig. 2d from Fig. 2c. Note T_A is estimated to be 3.45 K at 1.42 GHz.

Now our study is directed towards examine the accuracy of the system detector. This involves estimating *SNR* of the moon and sky background. The results are demonstrated in Fig. (4, and 5).

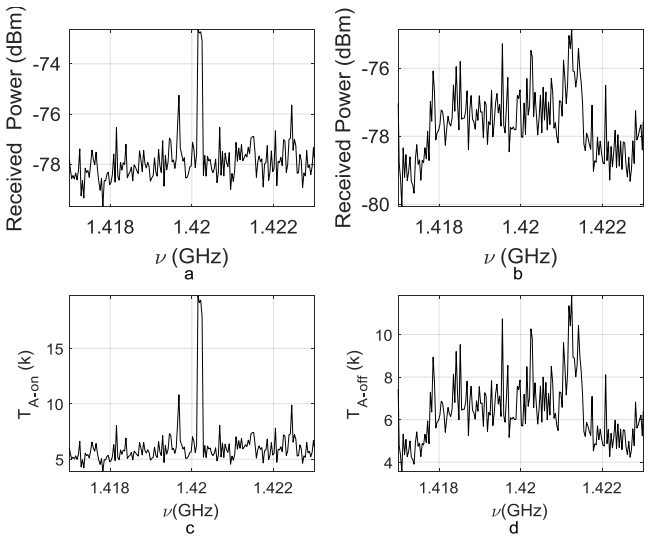

FIGURE 4: Received power (dBm) as a function of frequency *v* (GHz): a- Moon observation, b-Sky background observation, c- $T_{A\text{-}on}$ due to moon observation, d-$T_{A\text{-}off}$ due to sky background observation.

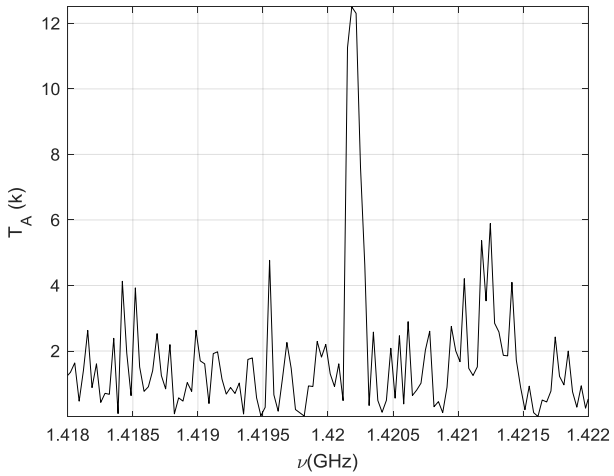

FIGURE 5: The result of subtracted Fig. 4d from Fig. 4c. Note T_A is estimated to be 12.5 K at 1.42 GHz.

It should be pointed out here that the result depicted in figure (5) is due to full moon observation.
SNR is then estimated to be the signal at around 1.42 GHz divided by the peak value of the sky background at the same frequency (*SNR* = 1.2).

Now our study is directed towards estimating the Half Power Beam Width (θ_{HPBW}) using the solar drift scan technique. In this case, the radio telescope antenna is kept stationary at west of an observed radio source position in the sky by a certain separation distance. This distance should be larger than the antenna beam width at less by five degrees. Using the rotation of earth to let the antenna beam drift steadily across the source, while the source pass over the beam width, then the received power is recorded.
The setting parameters that associated with this technique are Integration Bandwidth (Integ BW = 25 MHz), Channel Power Span (CH Pwr Span = 50 MHz). Then the antenna is fixed at (ϕ =154.3°, θ =51°) about 40 minute approximately until the sun crossed this position. The solar drift scan technique with a Gaussian function is made to fit the observed data. A Gaussian function is given by [22]:

$$G(x) = h \times exp\left[-\frac{(x-x_c)^2}{2\sigma^2}\right] \quad (13)$$

where h is the height of a Gaussian function, x is the observed data, σ is half width at half maximum, which equivalent to $\theta_{HPBW}/2$, and x_c is the central point of the function.
The results of the solar drift scan technique demonstrate in Fig. (6 and 7).

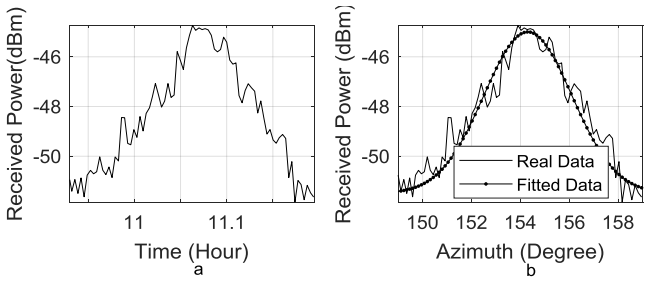

FIGURE 6: Solar drift scan technique and corresponding Gaussian fitting (March, 16, 2019), a – Received power (dBm) as a function of time (Hour), b–Received power (dBm) as a function of azimuth (Degree).

The values of the solar azimuth are taken from (Solar Position Algorithm) [23].
The elapsed time to cross the antenna beam width by the sun is approximately eighteen minutes and at this time the sun is crossed more than 5°. Fig. (7) describes fitted data to determine θ_{HPBW}.

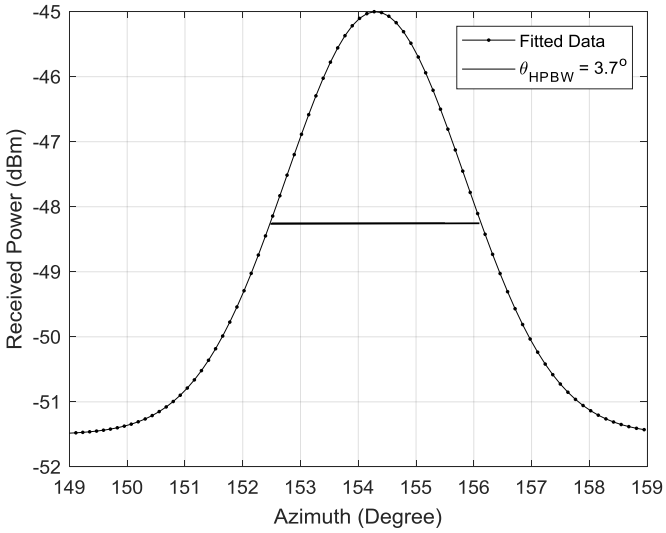

FIGURE 7: A fitted data of the solar drift scan technique.

θ_{HPBW} is estimated to be 3.7°.
The aperture efficiency (η) is estimated using Cas-A observation [24]:

$$\eta = \frac{2kT_A}{As} \quad (14)$$

T_A was estimated before (3.45 K), A is constant and equal 7.06 m^2 for our telescope, and the value of s is known to be 2477 Jy. Therefore, the aperture efficiency (η) is found to be 0.54.
Then A_e could be estimated using eq. (9), and found to be 3.8 m^2.
Finally, s_{min} is measured according to eq. (4), using T_{sys} = 64 K, A_e = 3.8 m^2, $\Delta\nu$ = 2×10^8 Hz, and τ = 30 second. Then found to be 0.9 Jy.
These computed results are compared with Jodrell Bank Internet Observatory of Manchester University, and with MIT Haystack observatory reports.

CONCLUSIONS

Several important points could be extracted from the results of this study

1. The estimated value (T_{sys}) of our radio telescope was found to be 64 K via eq. (11).
2. *SNR* is estimated to be 1.2. This value is obtained via full moon maximum peak temperature.
3. s_{min} is estimated to be 0.9 Jy according to eq. (4). This value demonstrates the ability of our radio detector to detect the minimum weak signals
4. θ_{HPBW} is measured by solar drift scan technique, and its estimated value (3.7°). This value is not violating the theoretical value (4.12°) that computed via eq. (5).
5. η, and A_e are estimated to be 0.54, and 3.8 m^2 respectively. These values are in a good agreement with the results presented in the literatures especially for small radio telescopes.

ACKNOWLEDGMENTS

We would like to express our thank and gratitude to the head of the department of Astronomy and Space, academic staff, colleagues and all friends at the College of Science, University of Baghdad for their valuable advices and encouragement.

REFERENCES

1. D. Smyth, *Handbook on Radio Astronomy*, ITU, Australia Radio Communication Bureau, 2013, Third Ed., 27.
2. E.L Daniyan, Int. J. Electron. Commun. **4**, No. (4): 461-471(2012).
3. G.A. Dulk, Ann. Rev. Astron. Astrophys. **23**:169-224(1985).
4. D. Oberoi, E.R. Evarts, and A.E. Rogers, Sol. Phys. **260**:389-400 (2009).
5. J. Cohen, T. Spoelstra, R. Ambrosini, and W. Driel, *CRAF Handbook for Radio Astronomy*, (European Science Foundation, 2005), Third Edition, pp. 31.
6. V.M. Nakariakov, L.K. Kashapova, Y.H Yan, Res. Astron. Astrophys. **14**(7) :1-6 (2014).
7. Deng Na, "High Resolution Studies of Complex Solar Active Region,", Ph.D. thesis, The State University of New Jersey, 2007.
8. Rauther A.S., Jangra S. International Journal of Scientific Research Engineering and Technology, **6**, Issue (6):589-599 (2017).
9. R.Anwar, N. Misran, M. Islam, and G. Gopir, J. Transact. Commun., **8**, Issue (8):755-764 (2009).
10. W. Wang, L. Xiao, and Y. Duan, Int. J. Ant. Propag., **2018** (1):1-17 (2018).
11. D.E. Gary, 2019. Radio astronomy Lecture 5. Physics 728.
12. K.O. Neil, "Single Dish Calibration Techniques at Radio Wavelength", in NAIC/NRAO school on Single Dish Radio astronomy- 2001. ASP Conference Series, **Vol. cs-278**, San Francisco, CA, pp. 1-18.
13. M. Weivaert, and Y. Rosseel, PLOS ONE J., **8**(11):1-11 (2014).
14. A. Narh., T. Quaye, F. Madjitey, P. Adzri, and E. Monorh, Res. J. Eng. App. Sci., **2**(4):262-266 (2013).
15. C. Chang, C. Monstein, A. Refregier, A. Amar, A. Glauser and S. Casura, ASP Conference Series, **Vol. 127** No. (957):1131-1143 (2015).
16. C.A. Balanis, *Antenna Theory Analysis and Design*, (John Wiley & Sons. Inc. Canada, 2005), Third edition, 106.
17. Uday E. Jallod, Kamal M. Abood. PIER Letter, **85**:17-24 (2019).
18. P. Ptatap, G. Mclntosh. Americ. Assoc. Phys. Teach., **73**(5): 399-404 (2005).
19. T.L Wilson., K. Rohlfs, S. Huttemeister**.** *Tools of Radio Astronomy*, *(*Springer-Verlag Berlin Heideelberg , 2013), Sixth edition, pp. 167.
20. J.W.M. Baars, R. Genzel, T. Pauliny, and A. Witzel, Astron. Astrophys. **61**:99-106 (1977).
21. T. Sage, M. Vidmar, J. Microelectron., Electron. Compon. Mater., **47**, No. 2 :113-128 (2017).
22. J.W. Goodman, *Statistical Optics*. (John Willy & Sons. Inc. New York, 2000), pp. 171.
23. Solar Position Algorithm (SPA) (http://midcdmz.nrel.gov/slops/spa.html).
24. V. Kalinov, Bulg. Astron. J., **15**:107-112 (2011).